

SUPPLEMENTAL DATA

A MODEL OF THE MEMBRANE-BOUND CYTOCHROME b_5 -CYTOCHROME P450 COMPLEX FROM NMR AND MUTAGENESIS DATA

Shivani Ahuja[†], Nicole Jahr[†], Sang-Choul Im[‡], Subramanian Vivekanandan[†], Nataliya Popovych[†], Stéphanie V. Le Clair[†], Rui Huang[†], Ronald Soong[†], Jiadi Xu[†], Kazutoshi Yamamoto[†], Ravi P. Nanga[†], Angela Bridges[‡], Lucy Waskell[‡] and Ayyalusamy Ramamoorthy[†]

TABLE S1. A comparison of the metabolism of methoxyflurane and benzphetamine by cytP4502B4 in solution and bicelles in the presence and absence of cytb₅. CytP4502B4 activity was stimulated 4.5-fold by cytb₅ in bicelles, albeit at only 33% of the activity in the aqueous control which contains DLPC. As a negative control, benzphetamine metabolism which, is not expected to be stimulated by cytb₅, was measured. We observed that benzphetamine metabolism was not stimulated by cytb₅ (as expected) and that cytP4502B4 benzphetamine activity was only decreased by a maximum of 30% when in the presence of bicelles.

[cytP450] (μM)	[DPC] (μM)	Bicelles [DMPC/DHPC] (mM)	nmoles F ⁻ /min/nmol cytP4502B4 or nmoles CH ₂ O/min/nmol cytP4502B4			Relative activity in micelles or bicelles
			-cytb ₅	+cytb ₅	+cytb ₅ / -cytb ₅	
Methoxyflurane metabolism						
1	-	-	0.19 ± 0.02	1.35 ± 0.04	7.1	100
1	500	-	0.22 ± 0.03	0.97 ± 0.02	4.4	72
1	1000	-	0.15 ± 0.04	0.63 ± 0.12	4.4	47
1	-	59.0/16.76	0.10 ± 0.02	0.45 ± 0.04	4.5	33
Benzphetamine metabolism						
0.2	-	-	46 ± 2	52 ± 2	1.1	100
0.2	200	-	30 ± 4	43 ± 5	1.4	83
0.2	-	36.88/10.47	33 ± 3	37 ± 5	1.1	71

TABLE S2. List of non-covalent interactions in clusters I and II obtained from HADDOCK. Non-covalent interactions were calculated using CCP4(1) and PISA (2).

Cluster I	cytb ₅		cytP450	
	residue	atom	residue	atom
hydrogen bonds	Asn62	HD22	Glu93	OE1
	Asn62	OD1	Lys433	HZ3
	Glu64	OD1	Arg126	HH11
	Asp65	OD1	Lys433	HZ1
	Asp65	OD2	Arg122	HH11
	His68	O	Arg126	HE
	His68	O	Arg126	HH21
	Ser69	OG	Leu129	O
	Asp71	N	Asp134	OD2
	Heme	O1A	Arg133	HH12
salt bridges	Glu64	OE1	Arg126	NH1
	Glu64	OE2	Arg126	NHE
	Glu64	OE2	Arg126	NH1
	Asp65	OD1	Lys433	NZ
	Asp65	OD2	Arg122	NH1
van der Waals	His31		Arg126	
	Phe63		Arg126	
	Val66		Lys433/Arg125	
	Gly67		Arg126	
	Thr70		Ala130/Asp134/Gly136	
	Ala72		Arg126	
	Arg73		Arg126	
	Glu74		Lys100	
	Heme		Arg125/Ile435	
Cluster II	cytb ₅		cytP450	
	residue	atom	residue	atom
hydrogen bonds	Glu48	OE1	Arg422	HH12
	Glu48	OE2	Arg422	HH22
	Glu49	OE2	Arg85	HH12
	Glu64	OE1	Arg126	HH22
	Glu64	OE2	Arg126	HH12
	Asp65	OD1	Lys433	HZ2
	Asp65	OD2	Arg122	HH11
	His68	O	Arg126	HE
	Ser69	OG	Arg133	HH22
	Asp71	OD2	Arg133	HH21
	Heme	O1A	Arg133	HH12

	Heme	O1D	Arg125	HE
	Heme	O2D	Arg125	HH21
salt bridges	Glu48	OE1	Arg422	NH2
	Glu48	OE1	Arg422	NH1
	Glu48	OE2	Arg422	NH2
	Glu48	OE2	Arg422	NH1
	Glu49	OE2	Arg85	NH1
	Glu49	OE2	Arg85	NH2
	Glu64	OE1	Arg126	NH1
	Glu64	OE1	Arg126	NH2
	Glu64	OE2	Arg126	NH1
	Glu64	OE2	Arg126	NH2
	Asp65	OD1	Lys433	NZ
	Asp65	OD2	Arg122	NH1
	Asp65	OD2	Arg122	NE
	Asp65	OD2	Lys433	NZ
	Asp71	OD2	Arg133	NH2
van der Waals	Gly47		Arg422	
	Val50		Val89	
	Asn62		Lys433	
	Phe63		Arg126	
	Val66		Arg125/Lys433	
	Gly67		Arg126	
	Thr70		Ala130	
	Arg73		Arg133	
	Heme		Leu129/Lys433	

FIGURE S1. (A) Sequence and secondary structure comparison of our NMR structure of cytb₅ (full-length) with other available NMR structures of cytb₅. Comparison to wild-type, truncated, ferric cytb₅ (unless otherwise noted) from the following species is presented: rabbit (1DO9) (3), human (2I96) (4), bovine (1HKO) (5), rat (1AW3) (6) and rat (reduced, 1AQA) (7). Secondary structure elements are color coded, with red for α -helices and blue for β -sheets. The sequence alignment was performed by Sequence Annotated by Structure (8). (B) Schematic representation of the sequential and medium range NOE connectivities involving NH, H α and H β protons. The thickness of the bars indicates the NOE intensities. The secondary structure of cytb₅ is shown for comparison.

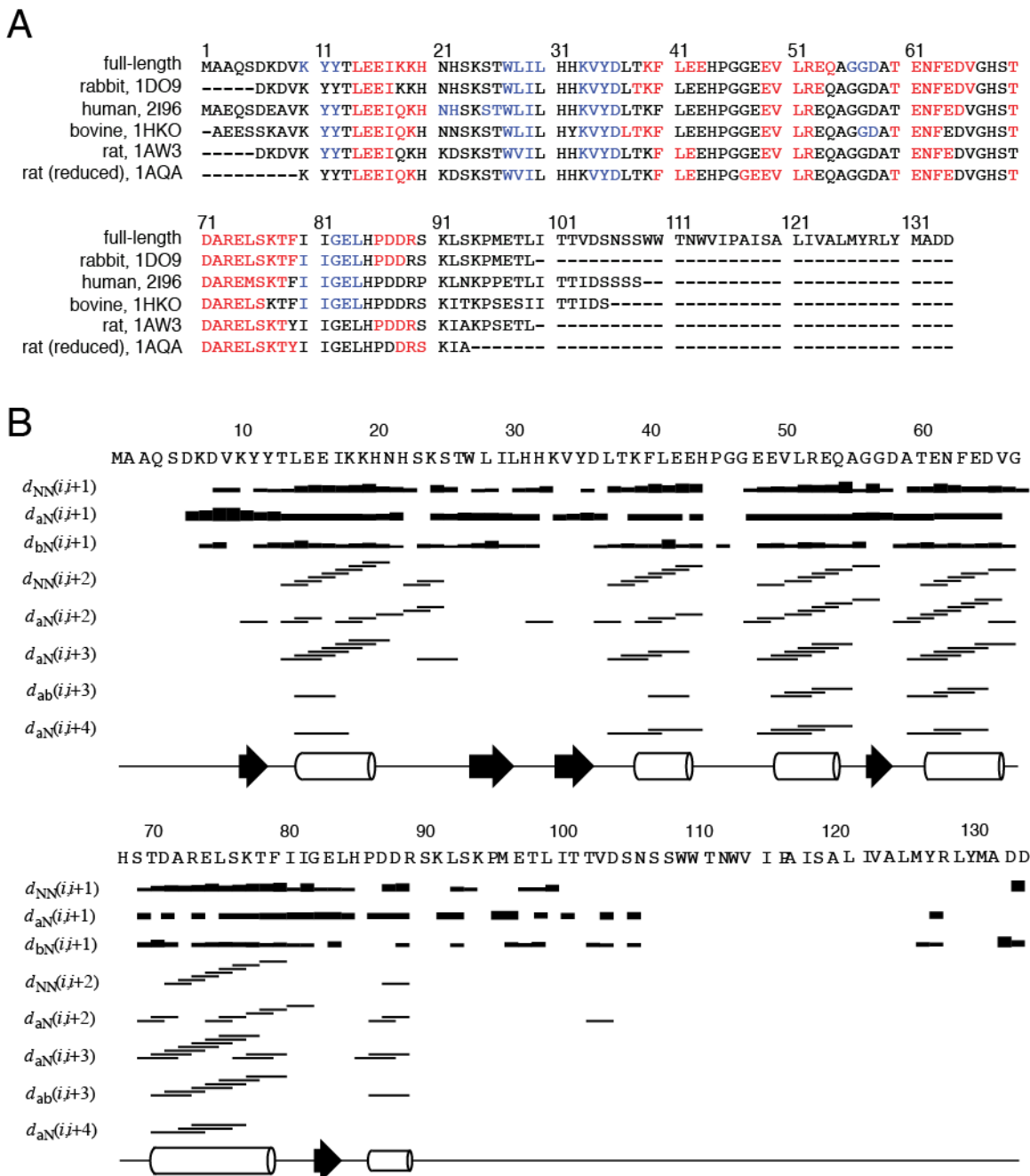


FIGURE S2. Interacting surfaces of cytb₅ and cytP4502B4. (A). Electrostatic potential surfaces for the high-resolution NMR structure of rabbit cytb₅ (top) and the X-ray crystal structure of the truncated heme-binding domain of rabbit cytP4502B4 (PDB code: 1SUO (9); bottom) generated using APBS software (10) and pdb2pqr server (11) in combination with PyMOL. The proximal surface of cytP450 (facing the viewer) contains the binding pocket for its redox partners. In the case of cytb₅, the electrostatic potential map shows a predominantly negatively charged surface (highlighted in red) that is expected to align with and bind to the positively charged surface on cytP4502B4 (highlighted in blue). (B) Amino acids selected for site-directed mutagenesis on cytb₅ and cytP450. A space filling model of cytb₅ (top) and cytP450 (bottom) shows the cytb₅ residues in green that were mutated in this study while the residues in orange on cytP450 were previously shown to be important for binding of cytb₅. The region of cytP450 colored a darker shade of grey represents the concave depression on the proximal surface of cytP450 that serves as the binding site for its redox partners (CPR and cytb₅) (12). The axial cysteine is shown in yellow. (C) And (D) are surface representations of the proximal side of cytb₅ (top) and cytP450 (bottom) generated from HADDOCK for clusters I and II, respectively. Residues that form the interaction interface are colored orange for cytb₅ and blue for cytP450.

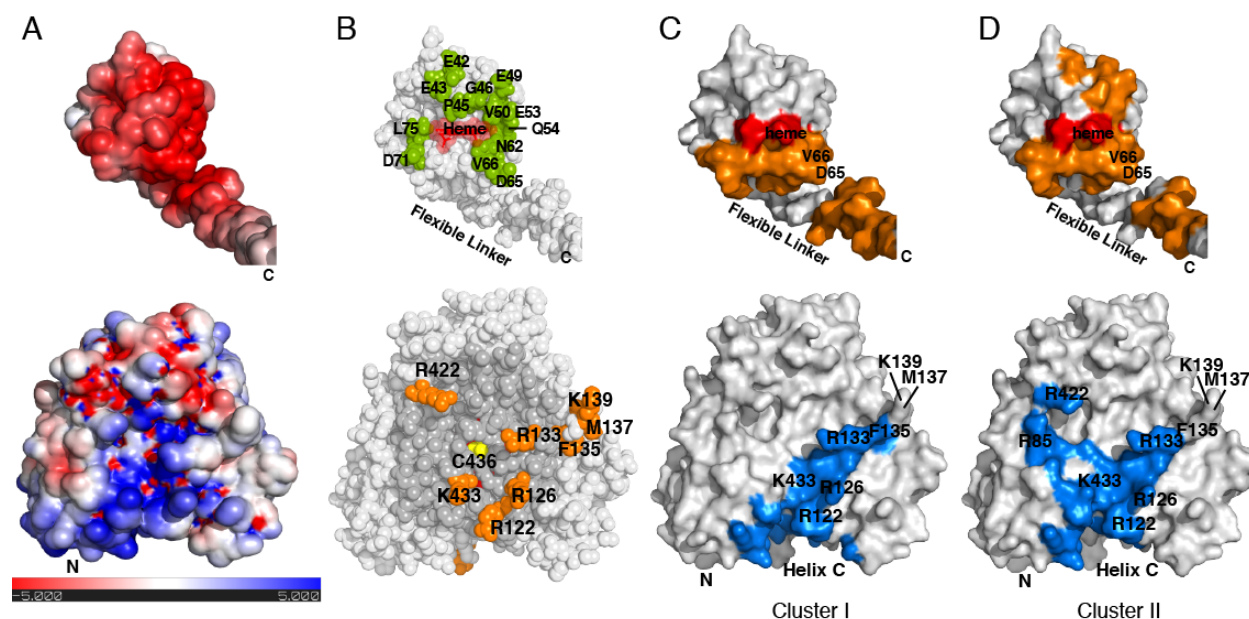
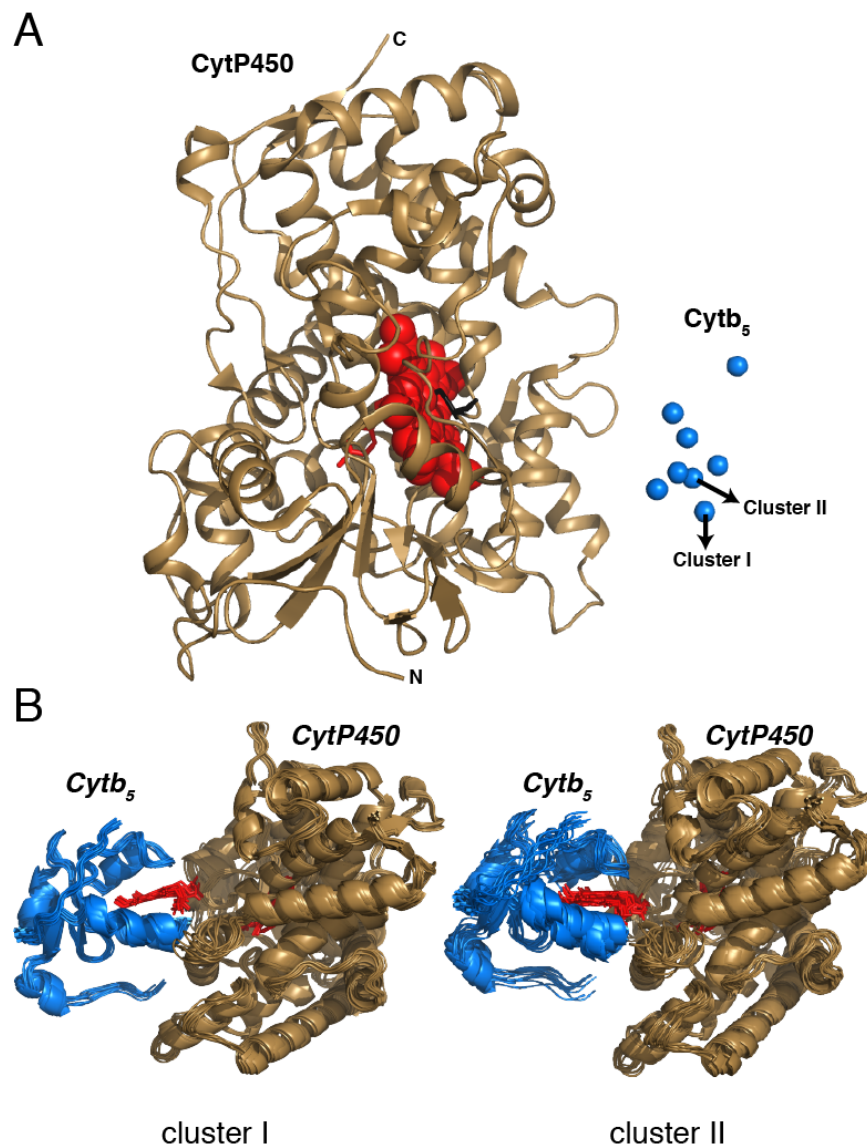


FIGURE S3. (A) Center of mass representation of the HADDOCK docking solution for the cytb_5 - cytP450 complex. The final 50 lowest energy complex orientations generated from HADDOCK were clustered based on the RMSD from a reference structure. 35 out of the 50 final structures were clustered into two main subpopulations (I and II), which are shown below and detailed in Figs. 7 and 8 and Table 6. However, the remaining 15 structures were further clustered into smaller groups based on RMSD from the reference structure. The figure here presents the center of mass (COM) of cytb_5 , presented in blue spheres, superimposed on the cartoon representation of cytP450 . The center of mass was calculated for one structure from each of the clusters representing the different complex orientations. Volkov *et. al.* (13) presented a similar depiction of a dynamic complex previously for the complex between soluble cytb_5 and cytc . (B) The two different clusters of cytb_5 - cytP450 complex structures obtained from HADDOCK. An overlay of the 10 lowest energy structures from the two main subpopulations (clusters I and II) of docked structures for the cytb_5 - cytP450 complex generated from HADDOCK.



ADDITIONAL REFERENCES

1. Potterton, E., Briggs, P., Turkenburg, M., and Dodson, E. (2003) A graphical user interface to the CCP4 program suite. *Acta Crystallogr. D Biol. Crystallogr.* **59**, 1131-1137
2. Krissinel, E., and Henrick, K. (2007) Inference of macromolecular assemblies from crystalline state. *J. Mol. Biol.* **372**, 774-797
3. Banci, L., Bertini, I., Rosato, A., and Scacchieri, S. (2000) Solution structure of oxidized microsomal rabbit cytochrome b5. Factors determining the heterogeneous binding of the heme. *Eur. J. Biochem.* **267**, 755-766
4. Nunez, M., Guittet, E., Pompon, D., van Heijenoort, C., and Truan, G. (2010) NMR structure note: oxidized microsomal human cytochrome b5. *J. Biomol. NMR.* **47(4)**, 289-295
5. Muskett, F. W., Kelly, G. P., and Whitford, D. (1996) The solution structure of bovine ferricytochrome b5 determined using heteronuclear NMR methods. *J. Mol. Biol.* **258**, 172-189
6. Arnesano, F., Banci, L., Bertini, I., and Felli, I. C. (1998) The solution structure of oxidized rat microsomal cytochrome b5. *Biochemistry* **37**, 173-184
7. Banci, L., Bertini, I., Ferroni, F., and Rosato, A. (1997) Solution structure of reduced microsomal rat cytochrome b5. *Eur. J. Biochem.* **249**, 270-279
8. Milburn, D., Laskowski, R. A., and Thornton, J. M. (1998) Sequences annotated by structure: a tool to facilitate the use of structural information in sequence analysis. *Protein Engineering* **11**, 855-859
9. Scott, E. E., White, M. A., He, Y. A., Johnson, E. F., Stout, C. D., and Halpert, J. R. (2004) Structure of mammalian cytochrome P450 2B4 complexed with 4-(4-chlorophenyl)imidazole at 1.9-A resolution: insight into the range of P450 conformations and the coordination of redox partner binding. *J. Biol. Chem.* **279**, 27294-27301
10. Baker, N. A., Sept, D., Joseph, S., Holst, M. J., and McCammon, J. A. (2001) Electrostatics of nanosystems: application to microtubules and the ribosome. *Proc. Natl. Acad. Sci. U. S. A.* **98**, 10037-10041
11. Dolinsky, T. J., Czodrowski, P., Li, H., Nielsen, J. E., Jensen, J. H., Klebe, G., and Baker, N. A. (2007) PDB2PQR: expanding and upgrading automated preparation of biomolecular structures for molecular simulations. *Nucleic Acids Res.* **35**, W522-W525
12. Bridges, A., Gruenke, L., Chang, Y. T., Vakser, I. A., Loew, G., and Waskell, L. (1998) Identification of the binding site on cytochrome P450 2B4 for cytochrome b5 and cytochrome P450 reductase. *J. Biol. Chem.* **273**, 17036-17049
13. Volkov, A. N., Ferrari, D., Worrall, J. A., Bonvin, A. M., and Ubbink, M. (2005) The orientations of cytochrome c in the highly dynamic complex with cytochrome b5 visualized by NMR and docking using HADDOCK. *Protein Sci.* **14**, 799-811